

Nonlinear Model Order Reduction and Control of Particle Size Distribution in a Semibatch Vinyl Acetate/Butyl Acrylate Emulsion Copolymerization Reactor

Myung-June Park and Francis J. Doyle III[†]

Department of Chemical Engineering, University of California, Santa Barbara, CA 93106, U.S.A.

(Received 28 October 2003 • accepted 12 December 2003)

Abstract—This paper addresses the control of the full particle size distribution (PSD) in a semibatch emulsion copolymerization reactor. The numerical approximation of a fundamental population balance model results in a high order system to accurately describe the distribution of particle size; therefore, model order reduction is required. Pseudo random input signals are input to the mechanistic model to generate a data set which covers the reachable region of the system, on the basis of which the transformation matrices are calculated by principal component analysis (PCA). A linear time varying model with reduced order obtained from the transformation matrices is augmented in the prediction equation of linear model predictive control. The performance of the controller is evaluated to drive the particle size distribution at the final time of the batch to the desired distribution in the presence of disturbances.

Key words: Particle Size Distribution, Model Order Reduction, Principal Component Analysis, Semibatch Emulsion Copolymerization Reactor

INTRODUCTION

The end-use quality of polymers produced by emulsion polymerization is highly dependent on the microstructural properties. For example, when the polymer latex is employed as paint, many of the end-use properties are directly related to the particle size distribution (PSD) of the polymer, while pressure sensitive adhesion is determined by the molecular weight distribution (MWD) [Elizalde et al., 2002]. Since a trial and error procedure is time consuming and is ineffective for the production of polymers with desired end-use property such as rheological properties and adhesion, research has been focused on the optimization and the control of the process on the basis of the available mathematical/mechanistic models. In order to describe the evolution of PSD in the emulsion polymerization, a population balance model [Ramkrishna, 2000] has been developed which includes the three major phenomena in the emulsion polymerization reactor: nucleation, growth and coagulation. Since Min and Ray [1974] introduced the modeling of the entire PSD, the population balance equation has been widely applied in the analysis of the emulsion polymerization reaction [Rawlings and Ray, 1987]. Coen et al. [1998] and Crowley et al. [2000] employed the zero-one modeling approach with the assumption that the particle population is classified into a population with zero radicals and a population with one radical, while Saldivar et al. [1998] applied a population balance equation to predict the PSD produced by micellar nucleation by making the pseudo-homopolymerization approximation. Zeaiter et al. [2002] modeled the semibatch emulsion polymerization reactor by using the zero-one model and the coagulation reaction based on DLVO theory. Immanuel et al. [2002] developed a mechanistic model in which the average number of

radicals per particle is calculated to account for the size-dependent growth rate and corroborated the effectiveness of the model by comparison with experimental data. In their recent work [Immanuel et al., 2003], they extended the model by including a coagulation mechanism.

As an analytical solution of the population balance model is obtained only under very strict assumptions, most solution methods are based on numerical analysis. The method of weighted residuals was described by Ramkrishna [1985], whereas Hounslow [1990] and Mantzaris et al. [2001] proposed a finite difference method (FDM) for the solution of discretized population balances. The FDM was also applied to an emulsion polymerization system [Gilbert, 1997]. Gelbard et al. [1980] and Langrebe and Pratsinis [1990] introduced the sectional model obtained by dividing the continuous PSD into a finite number of sections within which the size distribution function was assumed to be constant. Kumar and Ramkrishna [1997] discretized the distribution into classes of particles defined by finite particle size intervals and forced the discretization grid to move with particle growth rate in such a way that the partial differential equations were transformed from a differential to integral form over small intervals.

The control of polymer properties in emulsion polymerization has been studied by using several different strategies. Since Yabuki and MacGregor [1997] introduced the midcourse correction policy, this method was applied to the control of particle size distribution in the semibatch emulsion polymerization reactor by Flores-Cerrillo and MacGregor [2002]. Crowley et al. [2000] calculated the optimal input trajectory using sequential quadratic programming (SQP), while Immanuel and Doyle [2002] employed a genetic algorithm for the open-loop control of particle size distribution. As for feedback-based control, since a numerical solution technique for the time evolution of emulsion polymerization system (or any system whose dynamics are governed by a partial differential equation) necessitates the discretization of spatial variables, the order of the state in the corresponding control system becomes high. The

[†]To whom correspondence should be addressed.

E-mail: doyle@engineering.ucsb.edu

[‡]This paper is dedicated to Professor Hyun-Ku Rhee on the occasion of his retirement from the Seoul National University.

high dimensional model, however, is not directly amenable to dynamic analysis and model-based controller design. For example, high-order and ill-conditioning might render the corresponding linear control problems Riccati unsolvable [Su and Craig, 1991], and special numerical techniques may be needed to assess the basic properties of the models such as controllability and observability [Boley, 1994]. Valappil and Georgakis [2002] used an approximated mathematical model for emulsion styrene polymerization reactor and then controlled the end-use properties such as tensile strength and melt index by applying a nonlinear model predictive control based on the successive target region linearization method. Henson [2003] chose the finite elements as the outputs and controlled the cell distribution of yeast by using a linear time-varying model predictive control. Chiu and Christofides [1999] used the concept of inertial manifolds to reduce the model order. They applied the method of moments to a continuous crystallizer model and applied a nonlinear output feedback control algorithm.

An important principle that guides the present work is that the end-use properties are determined by the entire particle size distribution. Hence, the method of using lumped values, such as the moments, is not useful for the control of the entire size distribution. The system of our concern shows a bimodal distribution: one is the primary peak by the homogeneous nucleation and the other is the secondary peak by the micellar nucleation. Hence, the control aim in this paper is to regulate the entire particle size distribution. In order to reduce the order of the model, a principal component analysis (PCA) based model order reduction method is applied. For this purpose, the data set is generated by imposing a variety of input trajectories into the mechanistic (or the first principles) model for several batches. On the basis of the data at every sample time, the principal components (latent variables) and loading matrices are calculated and then these transformation matrices are applied to a linear time varying model produced by linearizing the nonlinear model along the nominal trajectory. The linear time varying model with reduced order is used in the application of a linear model predictive control to produce the polymer products with desired particle size distribution. In section 2, the mechanistic model is summarized and the model order reduction method is introduced in section 3, followed by section 4 in which the detailed procedure for the application of model order reduction method and the results of particle size distribution control in a semibatch emulsion vinyl acetate (VAc)/butyl acrylate (BuA) copolymerization reactor are discussed.

SEMIBATCH EMULSION COPOLYMERIZATION REACTOR MODEL

The mathematical model for the semibatch emulsion copolymerization reactor is summarized in this section. For further details about the model, the reader is referred to Immanuel et al. [2002] and Immanuel et al. [2003].

The evolution of particle size distribution in an emulsion polymerization is described by a population balance model of the following form:

$$\frac{\partial}{\partial t}F(r, t) + \frac{\partial}{\partial r}\left(F(r, t)\frac{dr}{dt}\right) = R_{nuc}(r, t) + R_{coag}(r, t) \quad (1)$$

where $F(r, t)$ denotes the particle density function. The second term

on the left-hand side, the partial derivative with respect to r , is the growth kernel, while R_{nuc} and R_{coag} represent the nucleation and coagulation reactions of particles with r size, respectively. Nucleation occurs by two methods: micellar nucleation and homogeneous nucleation. Micellar nucleation occurs when the concentration of free surfactant (S_w) in the aqueous phase exceeds the critical micelle concentration (cmc), whereas the oligomers in the aqueous phase with their length under the critical chain length (j_{cr}) aggregate surfactant molecules around them and bring about homogeneous nucleation. Thus, total nucleation rate is given by the combination of these two mechanisms:

$$R_{micellar} = \sum_{l=0}^{j_{cr}-1} \sum_{i=1}^2 e_{i,micelle}^l p_{wi} [P_w]^l C_{micelle} V_{aq} \quad (2)$$

$$R_{homogeneous} = k_{pav}^w [P_w^{j_{cr}-1}] V_{aq} \quad (3)$$

where $e_{i,micelle}^l$ and V_{aq} represent the entry rate constant for oligomers of type i and the volume of the aqueous phase, respectively. p_{wi} , $[P_w]^l$, and $C_{micelle}$ mean the probability of a radical of type i in the aqueous phase, the concentration of oligomer with chain length l in the aqueous phase, and the concentration of micelles, respectively.

Coagulation is explained by the thermodynamic instability of colloidal particles. The coagulation rate is composed of two terms: the formation of a particle by coagulation of particles and the depletion of a particle by coagulation with other particles:

$$R_{coag}(r, t) = H(r_{upper} - r) R_{formation}(r, t) - H(r_{cutoff} - r) R_{depletion} \quad (4)$$

Here, H is the Heaviside function which is unity when the argument is non-negative and zero otherwise. r_{cutoff} and r_{upper} represent the cut-off size below which the particles are prone to coagulate and the maximum size of particles that could result by the coagulation of smaller particles, respectively. The rate of formation is given by

$$R_{formation}(r, t) = \frac{1}{V_{aq}} \int \beta(r', r'') F(r', t) F(r'', t) \frac{r^2}{(r^3 - (r')^3)^{2/3}} dr' \quad (5)$$

and the rate of depletion is calculated as follows:

$$R_{depletion}(r, t) = \frac{1}{V_{aq}} \int_{r_{cutoff}}^{r_{max}} \beta(r, r') F(r, t) F(r', t) dr' \quad (6)$$

The intrinsic coagulation rate (coagulation kernel, β) is calculated by considering the forces and potentials between the particles:

$$\beta(r, r') = c_1 \frac{4\pi D_0 (r+r')}{W} \quad (7)$$

where D_0 is the diffusion coefficient and W denotes the Fuch's stability ratio.

The expression for the growth rate is a function of the particle radius (r):

$$R_{growth}(r, t) = \frac{dr}{dt} = \frac{3}{4\pi\rho_p} \sum_{i=1}^2 \sum_{j=1}^2 k_{pij} p_i \frac{\bar{n}(r, t)}{N_A} [M_j]_p MW_j \quad (8)$$

where k_{pij} , p_i , and $[M_j]_p$ denote the rate constant for propagation of polymer of type i with monomer j , the probability that a radical is

of type i in the particles, and the concentration of monomer j in the particles, respectively. $\bar{n}(r, t)$ and MW_j are average number of active radicals in particle of size r at time t and the molecular weight of monomer j , respectively.

In addition to the balance equation for the particle size distribution, mass balance equations for initiator, initiator radical and monomers are required. On the basis of the redox initiation system employed in the VAc/BuA copolymer system, the following material balances for the oxidizer (I_w), the reducer (Y_2) and the initiator radical (R_w) are calculated:

$$\frac{d([I_w]V_{aq})}{dt} = -k_{d1}[I_w][Y_1^r] + v_{I_w} \quad (9)$$

$$\frac{d([Y_2]V_{aq})}{dt} = -r_1 k_{d1}[I_w][Y_1^r] + v_{Y_2} \quad (10)$$

$$\begin{aligned} \frac{d([R_w]V_{aq})}{dt} = & k_{d1}[I_w][Y_1^r] - V_{aq} \sum_{i=1}^2 k_{ri}[R_w][M_i]_w \\ & - V_{aq} k_{t0}^w [R_w] \left(\sum_{l=0}^{j_i-1} [P_w]^l + [R_w] \right) \end{aligned} \quad (11)$$

Here, k_{d1} , r_1 and v_i denote the kinetic constants for the oxidation step, the stoichiometric ratio between the oxidizer and the reducer, and the molar feed rate of component i . $[Y_1^r]$ and $[M_i]_w$ represent the concentration of the catalyst in the reduced form and the concentration of monomer i in the aqueous phase.

The mass balance for the monomers is given by:

$$\begin{aligned} \frac{dM_j}{dt} = & v_{M_j} - \sum_{i=1}^2 (k_{pij}^w + k_{rij}^w) p_{wi} [\text{Oligomer}] [M_j]_w V_{aq} \\ & - \sum_{i=1}^2 (k_{pij} + k_{rij}) p_i [M_j]_p \int_{r=r_{nuc}}^{r_{max}} \bar{n}(r, t) F(r, t) dr \end{aligned} \quad (12)$$

where k_{pij}^w/k_{rij}^w and k_{pij}/k_{rij} are the rate constants in the particle/aqueous phases, for propagation and chain transfer to monomer, respectively, for a polymer of type i with monomer j and $[\text{Oligomer}] = \sum_{n=0}^{j_i-1} [P_w]^n$.

A great deal of research work has focused on developing solution techniques for distributed parameter systems [Ramkrishna, 1985]; and the ability to accurately solve population balance models has motivated numerous research studies on the dynamics of particulate processes. Among the variety of solution methods, discretization techniques are the most widely used. The finite difference method (FDM), one of the discretization methods, approximates the actual system by using finite differences in the spatial coordinate. This method, however, requires a great number of discrete points for an accurate solution and may result in spurious oscillations and numerical dispersion problems. Another method for the solution of the PBE is the method of weighted residuals (MWR). In this method, the weighted sum of the residuals within sub-domains is driven to zero. This method has a significant advantage over the FD method in that the numerical dispersion problem is overcome. According to the type of the basis function and weighting function used in the solution, the MWR is classified into the collocation technique and the Galerkin method. In the collocation method, an orthogonal polynomial is employed as the basis function while the Galerkin method uses a weighting function identical to the basis function.

In this study, the solution technology developed by Immanuel

and Doyle [2003] is applied. The continuous PSD is divided into a finite number of sections within which an integral quantity of the distribution is defined, in such a way that nucleation, growth and coagulation processes that occur in each of the sections are considered individually to update the particle count. Since this method determines the nucleation, growth and coagulation processes by the underlying thermodynamic and kinetic events, governed by relatively simple equations with relaxed stiffness characteristics, the associated stiffness in the full solution is removed. For details about the method, refer to Immanuel and Doyle [2003].

To discretize the population balance equation for the particle density function [cf. Eq. (1)], 250 elements (or grids) with a width of 2 nm are used and mass balance equations for the two monomers, aqueous phase volume, surfactant, oxidizer, reducer and initial radicals are calculated. Since the weight averaged particle size distribution (the controlled output) is calculated by using the particle density function as $wPSD(r, t) = r^3 F(r, t) / \sum_{i=1}^{250} r_i^3 F(r, t)$, it also is composed of 250 elements.

Fig. 1 shows the time evolution of particle density function every 12 min in a logarithmic scale. As depicted in the diagram, the differences of the magnitude of order between elements are so severe that the Jacobians become hypersensitive to slight changes in the variables. As a result, optimization based on gradient method is not applicable for the calculation of the optimal input values. Furthermore, as the magnitude changes very rapidly, it is difficult to find the bounds to normalize the variables.

NONLINEAR MODEL ORDER REDUCTION

As stated in the previous section, the approach commonly used in chemical engineering to address numerical solutions and control problems for distributed parameter systems is based on the finite discretization of the governing partial differential equations (PDEs). The discretization of the underlying conservation laws gives rise to dynamical systems of a very high order, often leading to ill-conditioned and uncontrollable systems.

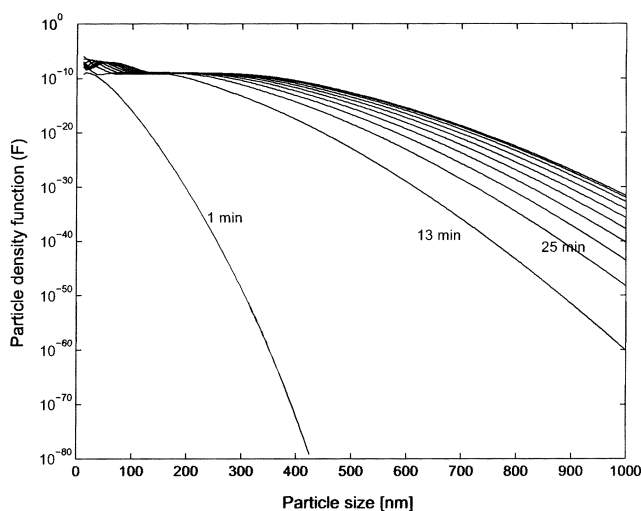


Fig. 1. Time evolution of the particle density function (nominal case) in increments of 12 minutes.

The main goal of a model order reduction (MOR) technique is to generate a model of the system with a reduced number of states while preserving accurately the behavior of the original (full order) system. In general, most MOR methods are based on the idea of projecting the full order states onto a state space with a suitable reduced order. For this purpose, the original states are changed to new states through a linear transformation:

$$\mathbf{x} = \mathbf{P}\mathbf{z} \quad (13)$$

where \mathbf{z} is a q -th order projection of state $\mathbf{x} \in \mathbb{R}^N$ in the reduced order state space and \mathbf{P} represents an orthonormal matrix for a transformation from the reduced one to the original state space.

Among the methods for the determination of the transformation matrix \mathbf{P} , the principal component analysis method (PCA) [Sharaf et al., 1986] is applied in the current work. The PCA is one of several multivariate statistical projection techniques in which the original number of (possibly) correlated variables is transformed into a (smaller) number of uncorrelated variables called *principal components*. With this technique, limitations due to measurement noise, correlated variables and unknown variables, and data set dimensionality can be solved. In addition, the technique removes numerical ill-conditioning from the data in an effort to make the highly sensitive system robust in the sense of resistance, that is, the ability of a procedure to display insensitivity to either small changes in most of the data or large changes in a small fraction of the data.

Before the PCA is applied, it is convenient to tailor the data in the calibration set in order to make the calculations easier [Geladi and Kowalski, 1986]. First, the values for each of the variables are transformed to mean-centered form. In the second step, variance scaling is used when the variables in a block are measured in different units: all the values for a certain variable are divided by the standard deviation for that variable in such a way that the variance for every variable is unity. In addition to these two scaling methods, one can give a smaller weight to certain variables of less importance.

Principal component analysis involves the expression of a matrix \mathbf{X} of rank r as a sum of r matrices of rank one:

$$\mathbf{X} = \mathbf{M}_1 + \mathbf{M}_2 + \dots + \mathbf{M}_r \quad (14)$$

These rank one matrices can all be written as outer products of two vectors; a score t_i and a loading p_i' :

$$\mathbf{X} = t_1 p_1' + t_2 p_2' + \dots + t_r p_r' \quad (15)$$

or equivalently $\mathbf{X} = \mathbf{TP}'$ (\mathbf{P}' is composed of the p' as rows and \mathbf{T} of the t as columns). The elements of the principal component are the direction cosines or the projections of a unit vector along the principal component on the axes of the plot. The scores vector (t_i) is a $n \times 1$ column vector (n : number of data). Its elements are the coordinates of the respective points on the principal component line. The scores and loadings can be calculated pair-by-pair by the non-linear iterative partial least squares (NIPALS) method [Sharaf et al., 1986].

Among all the principal components calculated by the PCA, only the first few PCs are used as shown in Eq. (15) as the other PCs are related to the noise. Too many PCs may cause collinearity problems. The number of principal components, a design variable that determines adequate description of the data, can be assessed by using a cross validation method. Ideally, the number of principal com-

ponents would be equal to the number of modes of variations present in the process. However, in practice, due to the inherent nonlinearity of the process and the measurement noise, more PCs may be needed to retain the relevant information present in the data matrix [Kesavan et al., 2000].

For nonlinear model order reduction, we consider the following nonlinear model:

$$\dot{\mathbf{x}} = \mathbf{f}(\mathbf{x}, \mathbf{u}) \quad (16)$$

The issues in applying the transformation matrix to a nonlinear system are associated with storage and evaluation. In order to transform the original nonlinear system to the reduced order system, one should evaluate the transformation matrix at every numerical integration step, which is computationally expensive. To solve this problem, a nonlinear model is linearized at every sample time by using a certain state (for example, a steady state in a continuous system, a nominal or initial point in a batch system) and a zero-order hold is used to calculate the discrete system matrices under the assumption that the state between sample times is not changed significantly. This is shown as follows:

$$\bar{\mathbf{x}}_{k+1} = \mathbf{A}_k \bar{\mathbf{x}}_k + \mathbf{B}_k \bar{\mathbf{u}}_k \quad (17)$$

$$\bar{\mathbf{y}}_k = \mathbf{H}_k \bar{\mathbf{x}}_k \quad (18)$$

where the overline denotes the deviation from the nominal state, and \mathbf{A}_k and \mathbf{B}_k are Jacobians of \mathbf{f} with respect to the state and input at step k . Higher order terms are assumed to be negligible.

The transformation matrix \mathbf{P} in Eq. (13) is applied to the linearized model, and consequently the following reduced order model is obtained:

$$\bar{\mathbf{z}}_{k+1} = \mathbf{A}_k' \bar{\mathbf{z}}_k + \mathbf{B}_k' \bar{\mathbf{u}}_k \quad (19)$$

$$\bar{\mathbf{y}}_k = \mathbf{H}_k' \bar{\mathbf{z}}_k \quad (20)$$

where $\mathbf{A}_k' = \mathbf{P}' \mathbf{A}_k \mathbf{P}$, $\mathbf{B}_k' = \mathbf{P}' \mathbf{B}_k$ and $\mathbf{H}_k' = \mathbf{H}_k \mathbf{P}$, respectively.

RESULTS AND DISCUSSION

1. Database Generation and Linear Transformation Matrix

In the basic steps of PCA, the generation of a database is the most crucial for the success of the procedure. However, there are no *a priori* comprehensive rules for the generation of the ensemble from which the orthogonal principal axes will be extracted [Shvartsman and Kevrekidis, 1998]. The data should be as completely representative of the region of concern as possible. Methods of forming a representative ensemble reported in the literature include the combination of spatiotemporal motions at several values of operating parameters [Bangia et al., 1997], mixing transients from initial conditions distributed randomly around the relevant regions of phase space [Graham and Kevrekidis, 1996], and strong responses to the perturbation of actuators from their nominal settings [Loffler and Marquardt, 1992; Aling et al., 1996].

In order to generate the database for the calculation of linear transformation matrices, pseudo random 4-level signals with switching probability of 7% are imposed on the plant (the first principles model) and the corresponding responses including state and output are saved in the database at every sample time (1 min). One of the manipulated variables is the flow rate of vinyl acetate feed with 0 and

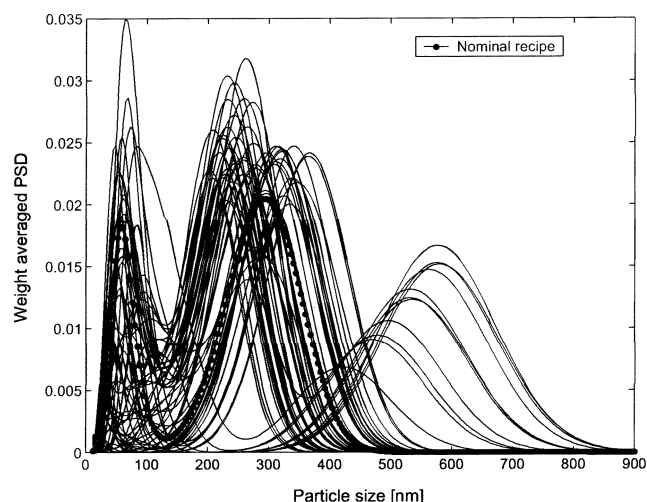


Fig. 2. Weight averaged particle size distribution at the final time generated by pseudo random 4-level signals (60 batches).

10.5 mol/s as low and high bounds, respectively, and the other is the feed flow rate of surfactant solution between 0 and 4.97 mol/s.

The reactor is initially charged with deionized water 1 L, VAc 52 g, ferrous ammonium sulphate (FAS) 0.1 g and sodium benzoate 1.12 g. The reaction temperature is assumed to be maintained at 60 °C. During the first 105 min, oxidizer (t-butyl hydrogen peroxide) and reducer (sodium formaldehyde sulfoxylate) are fed at a fixed rate of 2.71×10^{-4} and 1.86×10^{-4} mol/s, respectively and increased to 4.02×10^{-4} and 3.10×10^{-4} mol/s, respectively. The feed of BuA is injected at 2.81×10^{-4} mol/s for the first 90 min and then stopped until the end of the reaction.

Fig. 2 shows the results of weight averaged particle size distribution (wPSD) at the final time for 60 batches. Since the inputs are specified between the high and the low bounds, this figure accounts for the reachable region of the system under the current operation condition. During the early stage of the reaction, the amount of surfactant in the reactor does not reach the critical micelle concentration (cmc), so homogeneous nucleation occurs and the particles form the primary peak in the wPSD at final time. After the surfactant concentration exceeds the cmc, only micellar nucleation takes place in the reactor. It is observed in Fig. 2 that the primary peak has a separated region. This feature is explained by the effect of timing and amount of the initial surfactant feed flow rate. The primary peaks in the right-hand side (large particle primary peak region) are generated when the surfactant feed flow rate in the early stage is zero, while those in the middle are produced when the input for surfactant flow rate in the early stage has a value larger than zero. If the surfactant is not fed in the early stage, the micellar nucleation is delayed due to the lack of surfactant. Small numbers of micelles are responsible for the high monomer concentration in the particles and the high growth rate during that period, and consequently large particles are generated. Since the primary peak is highly sensitive to the amount and timing of the surfactant feed flow rate in the early stage, the continuous region would be observed if the input is changed more frequently (with high switching probability) and more input levels are used.

The differences of amplitude among the peaks in the large parti-

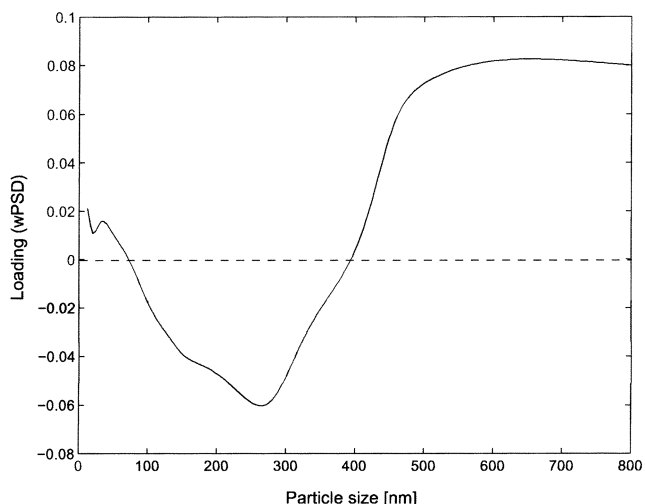


Fig. 3. Loading for the first principal component of weight averaged particle size distribution at final time.

cle primary peak region are attributed to the correlation of the micellar nucleation and the growth rate. If the rate of the micellar nucleation is high, the number of micelle is increased and thus, the monomer concentration in the particle and the growth rate become low. Therefore, the distribution which produces a primary peak of low amplitude in the large particle primary peak region has a secondary peak of high amplitude.

2. Application to an Emulsion Copolymerization Process

From the principal component analysis results in the previous section, linear time varying transformation matrices are determined. As discussed in the previous section, all the data are mean-centered and scaled to have unit variance. For the principal component analysis, the Statistics Toolbox for MATLAB is used. Among the state variables, the particle density functions and the weight averaged particle size distributions at all grids for 60 batches are used to calculate the transformation matrices at every sample time.

The results from the PCA reflect some of the characteristics of this system. Fig. 3 shows the loading that corresponds to the first principal component for the wPSD at final time. As observed in Fig. 3, the distribution in the small particle size has a different sign from that for the distribution in the large particle size, which means that the particles at each region have different sources: one from the homogeneous nucleation (large particle) and the other from the micellar nucleation (small particle). Since the first PC covers about 60% of total variances, the boundary for the different region in the loading does not match the real boundary in the observed data (*cf.* Fig. 2).

The input trajectories used in the generation of database are also analyzed by using PCA. The input values at every 12 min are selected for 60 batches and the loadings corresponding to the first PC for each input are presented in Fig. 4. As observed in the diagram, the elements of loadings in the early state have the same sign for the distribution in the large particle size. As homogeneous nucleation takes place in the early stage, the inputs during the first few minutes play a key role in controlling the peak by the homogeneous nucleation.

The upper diagram in Fig. 5 shows the number of principal com-

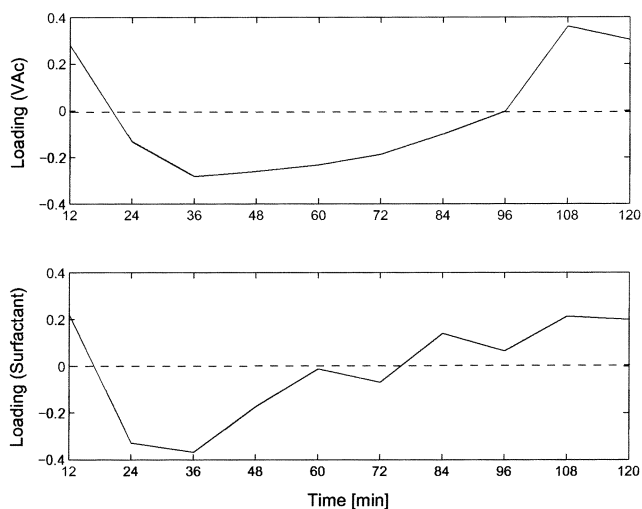


Fig. 4. Loading for the first principal component of inputs.

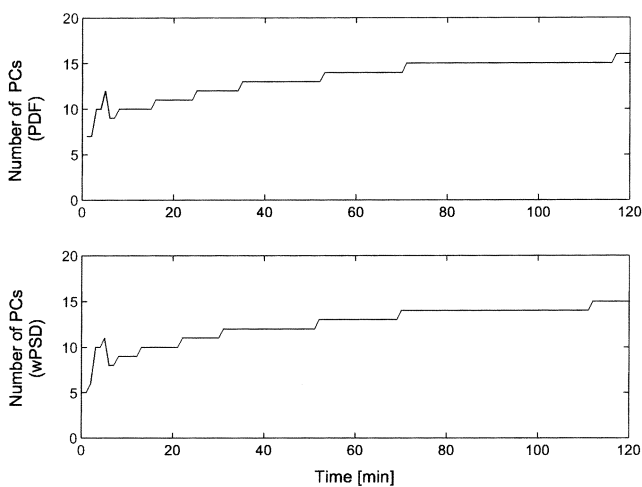


Fig. 5. Number of principal components covering 99.9% of total variance at each sample time.

ponents for the particle density function (F) with 99.9% cumulative variances at each sample time, respectively, while the lower diagram presents the number of PCs for the wPSD. Since the prediction of F with 90.0% cumulative variances shows disagreement with the observed value (*cf.* Fig. 6), the number of PCs is determined so that the transformation matrix should constitute more than 99.9% of total variances. It is worth emphasizing that the PCA approach described in this paper employs the nonlinear fundamental model directly, hence the unusually large variance is reasonable. If, on the other hand, data were employed to generate the PCs, a lower variance would be more practical to avoid capturing noise effects. The number of PCs for F is chosen with the largest value (16) at every sample time for the purpose of simplicity in constructing prediction equation. As for the wPSD, the number of PCs for 99.9% cumulative variances is determined as 15. It is noted that the state variables for mass balance equations, such as monomer concentration in the reactor, are not projected to the latent variable space but only the normalization is carried out as follows:

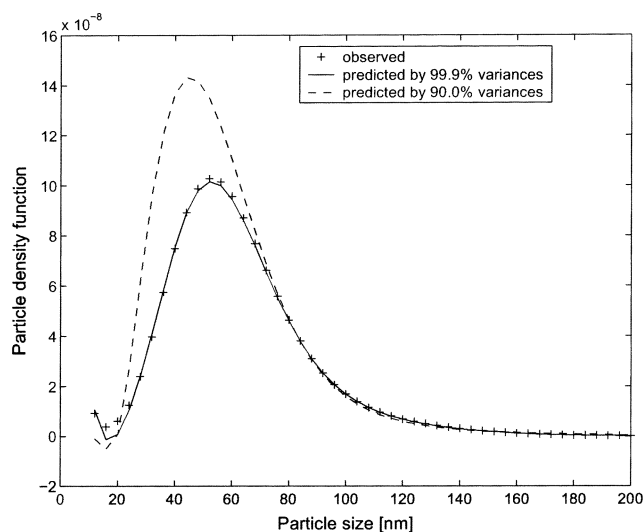


Fig. 6. Comparison between the prediction of particle density function by principal components and the observed data.

$$x_{normalized} = \frac{x - x_{min}}{x_{max} - x_{min}} \quad (21)$$

In general, the PCs for 80 or 90% variance predict the behavior of the original system in most of the results reported in the literature, while the PCs for 99.9% variance are needed in this system. This is because the measurement noise is not considered in the data set. If noise is present in the data set, a few dominant PCs will explain the behavior of the system and the others would be responsible for the measurement noise in such a way that fewer PCs will be needed.

After the transformation matrices are obtained, the reduced order model is used in the prediction equation of linear model predictive control (MPC) to build the prediction of future output behavior within a pre-specified horizon, called prediction horizon, in terms of current and future input moves within the control horizon. The prediction equation is used to construct the performance index, which is chosen to measure the output deviation from their respective reference values, and the optimization is performed to find a sequence of input moves that minimizes the performance index while satisfying all the given constraints. The model predictive control algorithm implements only the first of the calculated input sequences and the whole optimization is repeated at the next sampling time. A key feature contributing to the success of MPC is that various process constraints can be incorporated directly into the on-line optimization performed at each time step. Various versions of MPC based on the aforementioned principles have demonstrated their effectiveness in application to complex processes [Garcia and Morari, 1982; Lee and Ricker, 1994; Maner et al., 1996].

In the present system, the controller is applied to track the time-varying wPSD reference trajectory under the assumption that the state is available by state feedback. The prediction (p) and control (m) horizons are 10 and 5, respectively, and the sample time is 1 min. The weighting matrices for control error (Λ^y) and input (Λ^u) are $10 \times \mathbf{I}_{ny \times ny}$ and $\text{diag}([0.1, 0.52])$, respectively. The constraints on the input magnitude and the rate of input change are considered as follows:

Constraints on the input magnitude

$$0.0 \leq u_1 \leq 1.0 \times 10^{-3} \text{ [mol/s]}$$

$$0.0 \leq u_2 \leq 6.0 \times 10^{-3} \text{ [mol/s]}$$

Constraints on the rate of input change

$$-4.0 \times 10^{-4} \leq \Delta u_1 \leq 4.0 \times 10^{-4} \text{ [mol/s]}$$

$$-2.0 \times 10^{-3} \leq \Delta u_2 \leq 2.0 \times 10^{-3} \text{ [mol/s]}$$

Fig. 7 shows the wPSD at final time controlled by the linear MPC under nominal condition, and Fig. 8 presents the input profile calculated by the controller (solid line) and the nominal input profile (dashed line) used in the calculation of the time-varying wPSD reference trajectory. When the controller based on the original full order model is used, the closed loop system is hypersensitive to the change of variable or a slight deviation from the setpoint; thus the performance is not effective, even under the nominal case. As shown in

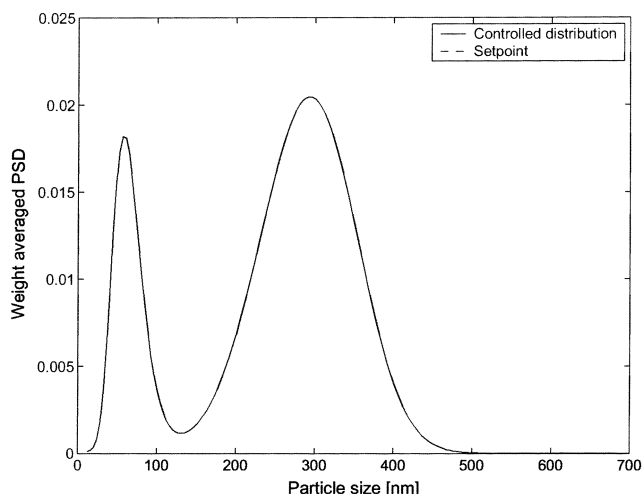


Fig. 7. Weight averaged particle size distribution at the final time controlled by the linear model predictive control on the basis of the reduced order model under nominal condition (controlled distribution and setpoint overlap each other).

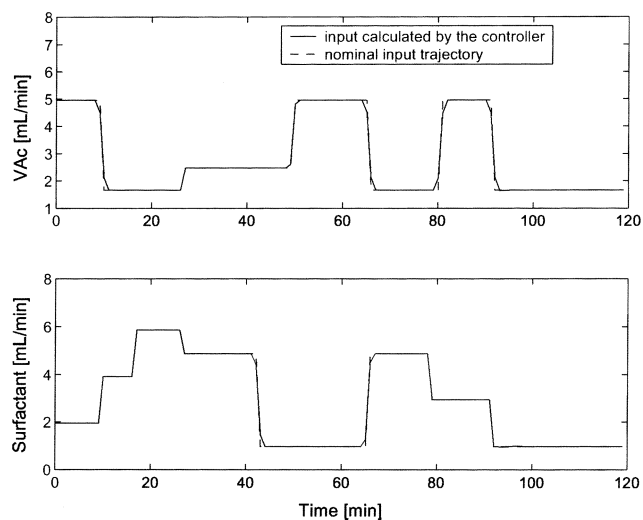


Fig. 8. Input profiles calculated by the controller under nominal condition and the nominal trajectories.

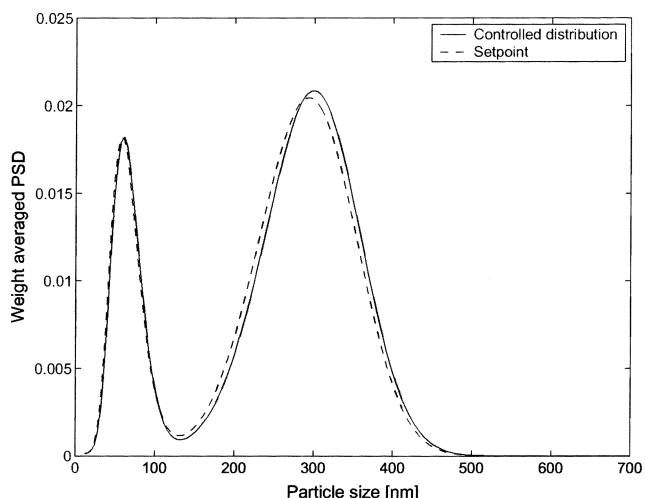


Fig. 9. Weight averaged particle size distribution at the final time controlled by the linear model predictive control on the basis of the reduced order model in the presence of disturbance (surfactant concentration).

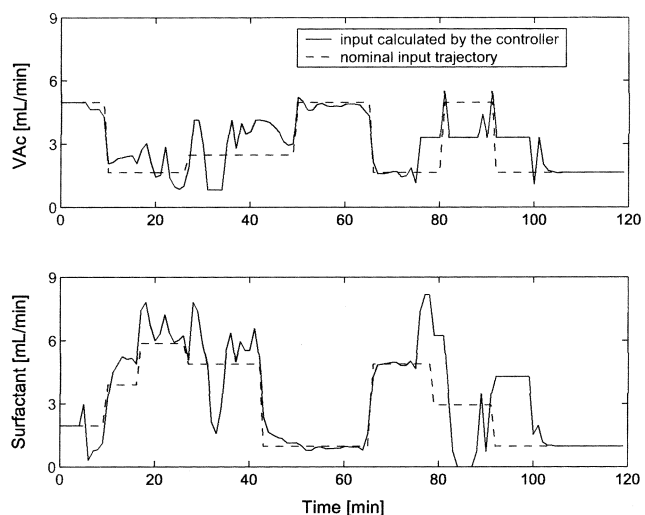


Fig. 10. Input profiles calculated by the controller in the presence of disturbance and the nominal input trajectories.

Figs. 7 and 8, the reduced order model yields a closed loop system that is well-conditioned and the performance is seen to be satisfactory.

To validate the performance of the controller for disturbance rejection, a disturbance is introduced to the surfactant concentration in the feed. The concentration in the plant is less than that in the model by 10% and the result is shown in Figs. 9 and 10. In this case, the prediction and the control horizons are increased to 25 and 15, respectively, to improve the performance of the controller and the weighting matrices are changed to $\Lambda^v = 8.1 \times 10^2 \mathbf{I}_{m \times m}$ and $\Lambda^u = \text{diag}([0.1, 1.1])$. Since the dynamic behavior of the system is determined in the early stage because of the characteristics of the batch reactor, the controller increases the feed flow rate of surfactant between 10 and 40 min to compensate for the error by the disturbance. Although the inputs show aggressive responses between 70 and 100 min to

eliminate the effect of the disturbance on the primary peak, the inputs finally converge to the nominal profile because the effect of the disturbance in the later stage of the reaction is not strong. At the final time, the controlled output shows a slight deviation but the error defined as

$$\frac{|\text{wPSD}_i(t_f) - \text{wPSD}_{i,\text{desired}}|^2}{|\text{wPSD}_{i,\text{desired}}|^2} \quad (22)$$

where $\|\cdot\|$ denotes the Euclidean norm is 1.84%. In summary, the disturbance rejection performance of the controller based on the reduced order model is shown to be quite good.

CONCLUSIONS

This article addresses the application of a model order reduction using principal component analysis to project a first principles model with high order onto the well conditioned latent variable space. The numerical solution of the population balance equation involves the discretization of the spatial coordinate, and thus the order of the system becomes high for the accurate prediction of the dynamic behavior of the system. In order to reduce the order of the original model, transformation matrices are calculated by using principal component analysis at every sample time from the data set generated by the responses of pseudo random multi-level input signals. Using these transformation matrices, the linear models obtained by the linearization of the original model along the nominal trajectory are transformed to the reduced order linear time-varying model. Since the number of the states and the outputs is reduced to less than 10% of the original order, and the magnitudes of order of latent variables are reasonable, the closed loop system becomes well conditioned in such a way that the controller developed by the reduced order model shows remarkable performance in controlling the entire particle size distribution both under the nominal case and in the presence of disturbance.

In our future work, the use of additional outputs such as total number of particles and solid content will be considered to improve the performance of the controller. In addition, the effectiveness of the transformation matrices will be corroborated under various types of disturbances in experimental studies, and the validity of the strategy to produce polymer product with a desired entire particle size distribution will be proven.

ACKNOWLEDGMENTS

This work was supported by the Post-doctoral Fellowship Program of the Korea Science and Engineering Foundation (KOSEF). The authors express their appreciation to Prof. Dale Seborg at the University of California, Santa Barbara for helpful advice with the work related to the principal component analysis.

REFERENCES

Aling, H., Ebert, J. L., Emami-Naeini, A. and Kosut, R. L., "Application of Nonlinear Model Reduction to Rapid Thermal Processing (RTP) Reactors," Proc. Int. Rapid Thermal Processing Conf., 356 (1996).
 Bangia, A. K., Batcho, P. F., Kevrekidis, I. G. and Karniadakis, G. E.,

"Unsteady 2-D Flows in Complex Geometries: Comparative Bifurcation Studies with Global Eigenfunction Expansions," *SIAM J. Sci. Comput.*, **18**, 775 (1997).
 Boley, D. L., "Krylov Space Methods on State-Space Control Models," *Circ. Syst. Signal Process*, **13**, 733 (1994).
 Chiu, T. and Christofides, P. D., "Nonlinear Control of Particulate Processes," *AIChE J.*, **45**, 1279 (1999).
 Coen, E. M., Gilbert, R. G., Morrison, B. R., Leube, H. and Peach, S., "Modeling Particle Size Distributions and Secondary Particle Formation in Emulsion Polymerization," *Polymer*, **39**, 7099 (1998).
 Crowley, T., Meadows, E., Kostoulas, E. and Doyle III, F. J., "Control of Particle Size Distribution Described by a Population Balance Model of Semibatch Emulsion Polymerization," *J. Proc. Control*, **10**, 419 (2000).
 Elizalde, O., Vicente, M., Leiza, J. R. and Asua, J. M., "Control of the Adhesive Properties of n-Butyl Acrylate/Styrene Latexes," *Polym. Reac. Eng.*, **10**, 265 (2002).
 Flores-Cerrillo, J. and MacGregor, J. F., "Control of Particle Size Distribution in Emulsion Semibatch Polymerization Using Mid-Course Correction Policies," *Ind. Eng. Chem. Res.*, **41**, 1805 (2002).
 Garcia, C. E. and Morari, M., "Internal Model Control: 1. A Unifying Review and Some New Results," *Ind. Eng. Chem. Process Des. Dev.*, **21**, 308 (1982).
 Geladi, P. and Kowalski, B. R., "Partial Least-Squares Regression: A Tutorial," *Anal. Chim. Acta*, **185**, 1 (1986).
 Gelbard, F., Tambour, Y. and Seinfeld, J. H., "Sectional Representation of Simulating Aerosol Dynamics," *J. Colloid Interface Sci.*, **68**, 363 (1980).
 Gilbert, R. G., "Emulsion Polymerization: A Mechanistic Approach," Academic Press (1995).
 Graham, M. and Kevrekidis, I. G., "Alternative Approaches to Karhunen-Loeve Decomposition for Model Reduction and Data Analysis," *Comp. Chem. Eng.*, **20**, 495 (1996).
 Henson, M. A., "Distribution Control of Particulate Systems Based on Population Balance Equation Models," Proc. Am. Control Conf., 3967 (2003).
 Hounslow, M. J., "A Discretized Population Balance for Continuous Systems at Steady-State," *AIChE J.*, **36**, 106 (1990).
 Immanuel, C. D. and Doyle III, F. J., "Open-loop Control of Particle Size Distribution in Semi-batch Emulsion Copolymerization Using a Genetic Algorithm," *Chem. Eng. Sci.*, **57**, 4415 (2002).
 Immanuel, C. D., Cordeiro, C. F., Sundaram, S. S., Meadows, E. S., Crowley, T. J. and Doyle III, F. J., "Modeling of Particle Size Distribution in Emulsion Co-polymerization: Comparison with Experimental Data and Parametric Sensitivity Studies," *Comp. Chem. Eng.*, **26**, 1133 (2002).
 Immanuel, C. D. and Doyle III, F. J., "Computationally-Efficient Solution of Population Balance Models Incorporating Nucleation, Growth and Coagulation: Application to Emulsion Polymerization," *Chem. Eng. Sci.*, **58**, 3681 (2003).
 Immanuel, C. D., Cordeiro, C. F., Sundaram, S. S. and Doyle III, F. J., "Population Balance PSD Model for Emulsion Polymerization with Steric Stabilizers," *AIChE J.*, **49**, 1392 (2003).
 Kesavan, P., Lee, J. H., Saucedo, V. and Krishnagopalan, G. A., "Partial Least Squares (PLS) based Monitoring and Control of Batch Digesters," *J. Proc. Control*, **10**, 229 (2000).
 Kumar, S. and Ramkrishna, D., "On the Solution of Population Balance

- Equations by Discretization-III. Nucleation, Growth and Aggregation of Particles," *Comp. Chem. Eng.*, **52**, 4659 (1997).
- Landgrebe, J. D. and Pratsinis, S. E., "A Discrete Sectional Model for Particulate Production by Gas Phase Chemical Reaction and Aerosol Coagulation in the Free Molecular Regime," *J. Colloid Interface Sci.*, **139**, 63 (1990).
- Lee, J. H. and Ricker, N. L., "Extended Kalman Filter Based Nonlinear Model Predictive Control," *Ind. Eng. Chem. Res.*, **33**, 1530 (1994).
- Loffler, H. P. and Marquardt, W., "On the Order Reduction of Nonlinear Differential-Algebraic Process Models," *Proc. Am. Control Conf.*, 1546 (1992).
- Maner, B., Doyle III, F. J., Ogunnaike, B. A. and Pearson, P. K., "Nonlinear Model Predictive Control of a Multivariable Polymerization Reactor Using Second-Order Volterra Series," *Automatica*, **32**, 1285 (1996).
- Mantzaris, N. V., Daoutidis, P. and Sriece, F., "Numerical Solution of Multivariable Cell Population Balance Models. Parts: I, II and III," *Comp. Chem. Eng.*, **25**, 1411 (2001).
- Min, K. W. and Ray, W. H., "On the Mathematical Modeling of Emulsion Polymerization Reactors," *J.M.S.-Review Macromolecular Chemistry*, **C11**, 177 (1974).
- Ramkrishna, D., "The Status of Population Balances," *Rev. Chem. Eng.*, **3**, 49 (1985).
- Ramkrishna, D., "Population Balances," Academic Press, San Diego (2000).
- Rawlings, J. B. and Ray, W. H., "Stability of Continuous Emulsion Polymerization Reactors: a Detailed Model Analysis," *Chem. Eng. Sci.*, **42**, 2767 (1987).
- Saldivar, E., Dafniotis, P. and Ray, W. H., "Mathematical Modeling of Emulsion Copolymerization Reactors. I. Model Formulation and Application to Reactors Operating with Micellar Nucleation," *J.M.S.-Review Macromolecular Chemistry*, **C38**, 207 (1998).
- Sharaf, M. A., Illman, D. L. and Kowalski, B. R., "Chemometrics," John Wiley & Sons, New York (1986).
- Shvartsman, S. Y. and Kevrekidis, I. G., "Nonlinear Model Reduction for Control of Distributed Systems: A Computer-Assisted Study," *AIChE J.*, **44**, 1579 (1998).
- Su, T. and Craig, Jr., P. R., "Model Reduction and Control of Flexible Structures Using Krylov Vectors," *J. Guid. Control Dynam.*, **14**, 260 (1991).
- Valappil, J. and Georgakis, C., "Nonlinear Model Predictive Control of End-Use Properties in Batch Reactors," *AIChE J.*, **48**, 2006 (2002).
- Yabuki, Y. and MacGregor, J. F., "Product Quality Control in Semibatch Reactors Using Midcourse Correction Policies," *Ind. Eng. Chem. Res.*, **36**, 1268 (1997).
- Zeaiter, J., Romagnoli, J. A., Barton, G. W., Gomes, V. G., Hawkett, B. S. and Gilbert, R. G., "Operation of Semi-batch Emulsion Polymerisation Reactors: Modeling, Validation and Effect of Operating Conditions," *Chem. Eng. Sci.*, **57**, 2955 (2002).